Atomic Mapping of the Sugar Interactions in One-Site and Two-Site Mutants of Cyanovirin-N by NMR Spectroscopy[†]

Corine Sandström,*[,‡] Birgit Hakkarainen,[‡] Elena Matei,[§] Anja Glinchert,[||] Martina Lahmann,[⊥] Stefan Oscarson,[||] Lennart Kenne,[‡] and Angela M. Gronenborn[§]

Department of Chemistry, Swedish University of Agricultural Sciences, P.O. Box 7015, SE-750 07 Uppsala, Sweden, Department of Structural Biology, University of Pittsburgh School of Medicine, Pittsburgh, Pennsylvania 15261, Centre for Synthesis and Chemical Biology, University College Dublin, Belfield, Dublin 4, Ireland, and The School of Chemistry, University of Bangor, Alun Roberts Building, Deiniol Road, Bangor, Gwynedd LL57 2UW, U.K.

Received November 2, 2007; Revised Manuscript Received January 23, 2008

ABSTRACT: The details of the interaction between two mutants of Cyanovirin-N (CV-N), an HIV inactivating protein, and di- and trimannosides, substructures of Man-9, were investigated by STD NMR spectroscopy. One mutant, CV-N^{mutDB}, contains only one carbohydrate-binding site on domain A, whereas in CV-N^{mutDA}, the specificity of domain A for trimannose was changed while the site in domain B was kept intact, allowing for a dissection of the overall binding. Results of the STD NMR experiments revealed close contact between the protein binding site on domain A and H2, H3, and H4 of the nonreducing terminal mannose unit for Manα(1–2)Manα*O*Me, Manα(1–2)Manα(1–3)Manα*O*Me, and Manα(1–2)-Manα(1–6)Manα*O*Me. The Manα(1–2)Manα(1–2)Manα*O*Me trisaccharide interacted with CV-N with the highest affinity. Further dissection of the interaction was achieved by NMR experiments with synthetic 2′-, 3′-, 4′-, and 6′-deoxy analogues of the disaccharide Manα(1–2)Manα*O*Me. STD and $^{1}H-^{15}N$ HSQC NMR spectroscopy revealed that the 2′- and 6′-deoxy dimannosides were recognized by CV-N, whereas no binding was detected for the 3′- and 4′-deoxy sugars. These results demonstrate that the 3′- and 4′-hydroxyl groups on the terminal residue are engaged in key polar interactions with the protein and are required for high-affinity binding.

Cyanovirin-N (CV-N) is an 11 kDa protein that was originally isolated from aqueous extract of the cyanobacterium *Nostoc ellipsosporum* (*1*). CV-N has a broad antiviral activity, and it irreversibly inactivates diverse laboratory strains and isolates of human immunodeficiency virus (HIV) as well as a variety of other enveloped viruses such as Ebola, human herpes virus 6, measles viruses, and hepatitis C (*1–6*). In the case of HIV, the antiviral activity of CV-N is mediated through high-affinity interactions with the viral surface envelope glycoproteins. More specifically, CV-N acts by binding to high-mannose oligosaccharides on gp120, Man-8 and Man-9 (Scheme 1), and exerts its activity at nanomolar concentrations (*1, 4, 7–9*).

Several three-dimensional (3D) structures of CV-N have been determined by NMR and X-ray crystallography (*10–15*), and two carbohydrate binding sites separated by ∼40 Å have been identified on the protein (*12, 16*). Site 1 on domain B (residues 39–89) is a deep pocket, while site 2 on domain A (residues 1–38 and 90–101) is a shallow cleft. Binding studies using isothermal titration calorimetry (ITC) and NMR indicated that for both sites, the minimum molecule required for binding is the disaccharide Manα(1–2)Man (*16, 17*). In the bound form, both mannopyranose rings of the sugar keep the chair conformation, and the nonreducing pyranose ring is stacked over the original reducing mannopyranose ring (*12, 14*). Different affinities for the Manα(1–2)Man disaccharide and the trisaccharides forming the three arms of Man-9 (Scheme 1) were noted (*14, 18*), with domain A exhibiting a slight preference for the trimannoside Manα(1–2)-Manα(1–2)Man and domain B for the dimannoside Manα-(1–2)Man. In all cases, the reported binding constants were similar and in the micromolar range (*16–18*).

To improve our understanding of the structural basis of interaction of carbohydrate with CV-N, we performed saturation transfer difference (STD) NMR experiments (*19–23*) on these di- and trisaccharides together with CV-N for measurement of the protein−sugar complexes (*24*). Epitope mapping for the disaccharide Manα(1–2)Manα*O*Me obtained by STD NMR (*24*) was in good agreement with previous results. Experiments with the trisaccharides revealed for the first time that a (1–2) linkage between the mannose located at the nonreducing end and the penultimate residue was important for recognition. The Manα(1–2)Manα*O*Me disaccharide and the Manα(1–2)Manα(1–3)Manα*O*Me and Manα(1–2)Manα(1–6)Manα*O*Me trisaccharides exhibited STD NMR spectra clearly different from that of the all (1–2)-linked Manα(1–2)Manα(1–2)Manα*O*Me, suggesting that

[†] This work was supported by the Swedish Research Council, by grants from EU (MRTN-CT-2004-005645 GlycoGold), and by grants from the Commonwealth of Pennsylvania.

* To whom correspondence should be addressed. Phone: (+46) 18 67 22 17. Fax: (+46) 18 67 34 76. E-mail: corine.sandstrom@kemi.slu.se.

[‡] Swedish University of Agricultural Sciences.

[§] University of Pittsburgh School of Medicine.

[||] University College Dublin.

[⊥] University of Bangor.

10.1021/bi702200m CCC: $40.75
Published on Web 03/01/2008

Scheme 1: Chemical Structures of $Man_9GlcNAc_2$, Disaccharide **1**, and Trisaccharides **2**−**5**

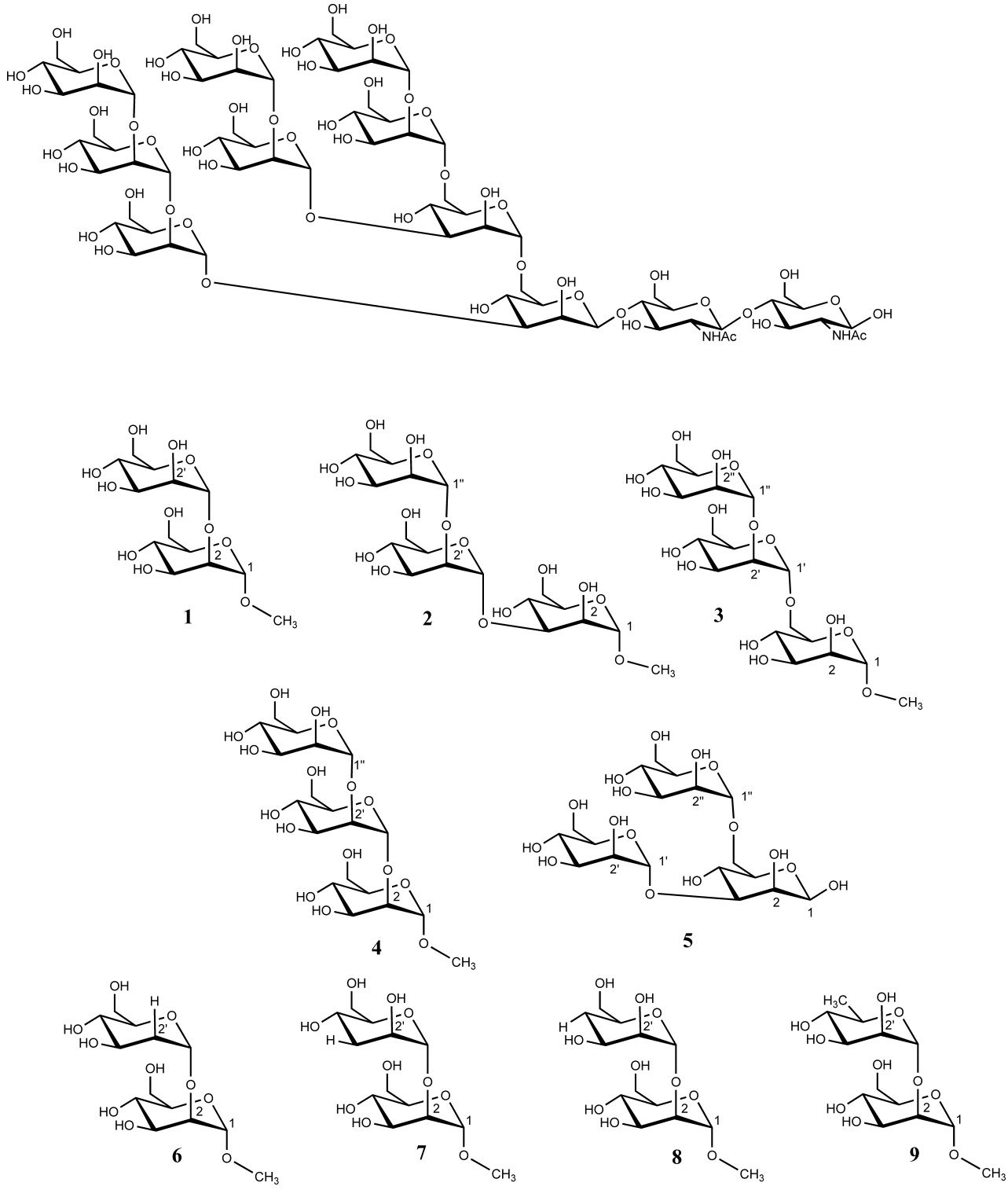

CV-N is capable of discriminating between structurally similar compounds.

However, since CV-N contains two binding sites that can simultaneously be occupied in solution, only an average picture of the interacting sugar epitopes was obtained from the initial STD NMR data. To differentiate between the two protein binding sites, we designed protein variants in which the binding sites were either obliterated (CV-N^{mutDB}) or changed (CV-N^{mutDA}) (*25*) (Scheme 2). In the CV-N^{mutDB} mutant, the binding site on domain B^M that showed a slight preference for the dimannoside Manα(1–2)Manα was abolished. For CV-N^{mutDA}, instead of completely abolishing the binding site on domain A^M, we changed the primary sequence of amino acids to make this domain more similar to that of domain B^M. Such modification suppressed the preference for the trimannoside while preserving the ability to recognize the Manα(1–2)Manα epitope. Therefore, in CV-N^{mutDB}, only a single binding site remains, allowing a direct and unambiguous investigation of sugar binding to this site without any complications associated with exchange or other conformational heterogeneity associated with a two-site interaction. In this manner, it is possible to precisely define the

Scheme 2: Schematic Representation of the Mutants CV-N^{mutDA} and CV-N^{mutDB} [a]

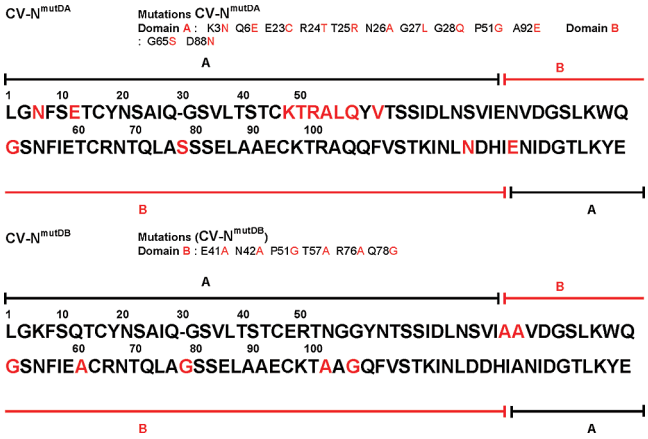

[a] The amino acid sequence is aligned to highlight the amino acid repeat in wild-type CV-N. All changes in residues are colored red.

contact epitope on the sugar for this binding site of the protein by STD NMR. Here, we present such data for the interactions of the mutant proteins with the synthetic di- and trimannoside substructures of Man-9.

Hydrogen bonds by hydroxyl groups of sugars are assumed to play a crucial role in lectin−carbohydrate interaction and frequently contribute to both specificity and affinity. Using deoxy sugar analogues of Manα(1–2)Manα*O*Me, we have identified, by STD and $^{1}H-^{15}N$ HSQC chemical shift mapping NMR experiments, the key hydroxyls on the sugars that are pertinent to the CV-N−oligomannoside binding.

RESULTS

*STD NMR Experiments and Epitope Mapping of Disaccharide **1** and Trisaccharides **2–5** Interacting with CV-N^{mutDA} and CV-N ^{mutDB}.* Figure 1 displays the reference proton STD NMR spectra of Manα(1–2)Manα*O*Me (m2m, **1**) alone and in the presence of CV-N^{mutDA} and CV-N^{mutDB}. In the STD NMR spectra recorded for samples containing the ligands only, traces of the reference one-dimensional (1D) NMR spectra were observed. Therefore, these spectra were corrected by subtracting protein-only STD NMR spectra obtained under identical experimental conditions. The corrected spectra exhibited large signals, demonstrating that the disaccharide binds to both mutants. In general, magnetization transfer from the protein to the ligand correlates with the proximity of ligand atoms and the protein, resulting in the strongest STD signals for close contacts. For both CV-N variants investigated here, the largest STD effects are observed for H2′, H3′, and H4′ on the nonreducing end sugar, indicating that these protons are in closest contact with the proteins. Enhancement is also seen for the H4 resonance on the original reducing end residue. Relative to the *O*Me group, the STD effects are larger for m2m **1** in the presence of CV-N^{mutDB} than in presence of CV-N^{mutDA} (Figure 1).

The STD NMR spectra (see the Supporting Information) of Manα(1–2)Manα(1–3)Manα*O*Me (m2m3m, **2**) and of Manα(1–2)Manα(1–6)Manα*O*Me (m2m6m, **3**) in the presence of CV-N^{mutDA} and CV-N^{mutDB} also showed that binding occurred. As seen with the 1,2-linked disaccharide **1**, the signals with the highest intensities were observed for H2″, H3″, and H4″ of the terminal, nonreducing mannose unit, as well as for H4′, indicating that these protons are in intimate contact with the protein. No STD effects were observed for protons located on the original reducing end mannose residue, suggesting that this sugar is farther from the protein binding site. The STD NMR spectra of m2m3m, **2**, were very similar for both mutants, while those of m2m6m, **3**, exhibited smaller STD effects in the presence of CV-N^{mutDA} than in the presence of CV-N^{mutDB}.

For the all 1,2-linked trisaccharide m2m2m, **4** (Figure 2), and the branched trisaccharide Manα(1–3)[Manα1–6]-Manα*O*Me, m(m3)6m, **5** (Supporting Information), no STD effects were observed. The absence of STD signals can be caused by two scenarios: (i) no interaction between the ligand and the protein or (ii) slow exchange between the bound and free state of the ligand (high-affinity binding). To evaluate whether tight binding may be the cause of the lack of STD signals with the two trisaccharides, we performed competition STD NMR (*22, 26*) experiments. In these experiments, high-affinity binding can be indirectly detected by monitoring the STD signals of a known low-affinity ligand, if the high-affinity ligand interacts with the same binding site as the low-affinity ligand. In that case, a decrease in intensity or disappearance of the STD signals of the lower-affinity ligand is observed.

We selected the disaccharide m2m, **1**, and the trisaccharide m2m6m, **3**, as low-affinity ligands since strong STD signals were obtained for both with the two mutants. Upon addition of an equimolar amount of the core trisaccharide m(m3)6m, **5**, the STD NMR spectra of m2m6m, **3** (Supporting Information), remained almost unchanged and no new signals from m(m3)6m, **5**, appeared, demonstrating that this compound did not bind to the CV-N variants. This result is in accord with previous studies that showed no interaction between the Man-9 core trisaccharide and wild-type CV-N (*17*). We thus conclude that the terminal Manα(1–2)Manα unit is also the main epitope for binding to the mutant CV-N forms.

Figure 3 shows the STD NMR spectra of m2m, **1**, in competition with m2m2m, **4**. In this case, the addition of an equimolar amount of m2m2m, **4**, resulted in a large decrease in the intensities of the STD signals of **1** for both mutant proteins. This demonstrates that m2m, **1**, and m2m2m, **4**, compete for the same binding sites on CV-N and the mutants. The result also confirms that the trisaccharide m2m2m exhibits a higher affinity than the disaccharide m2m. The equivalent experiments performed with m2m6m, **3**, in competition with m2m2m, **4**, also caused an intensity decrease of the STD signals of m2m6m, **3** (spectra not shown), corroborating that the all 1,2-linked trisaccharide interacts with the proteins.

*STD NMR Experiments with 2′-, 3′-, 4′-, and 6′-Deoxy Analogues (**6**−**9**, respectively) of Manα(1–2)Manα*OMe.* On the basis of STD NMR results that identified H2, H3, and H4 on the nonreducing end sugar ring as close contact points with the protein, we synthesized 2′-, 3′-, 4′-, and 6′-deoxy analogues of the disaccharide Manα(1–2)Manα*O*Me (Scheme 1) and investigated their binding to the two CV-N mutants.

The STD NMR spectra (Figure 4) clearly showed that the 6′-deoxy disaccharide, **9**, binds to the two mutants in a similar manner as the sugar that carries a hydroxyl group at the 6′ position. As with Manα(1–2)Manα*O*Me, the strongest STD

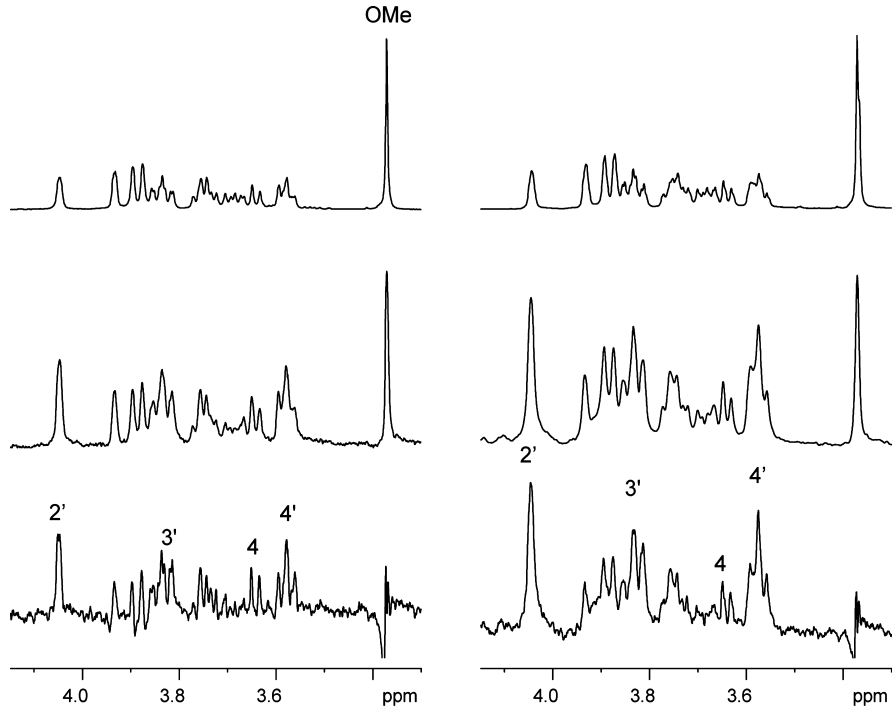

FIGURE 1: 1D ^{1}H NMR spectra of disaccharide m2m, **1**, at 600 MHz and 10 °C in the presence of CV-N^{mutDA} (left) and CV-N^{mutDB} (right). Reference NMR spectra (top), STD NMR spectra (middle), and "cleaned" STD NMR spectra obtained by subtracting the ligand-only STD NMR spectra from the spectrum obtained in the presence of protein (see Experimental Procedures).

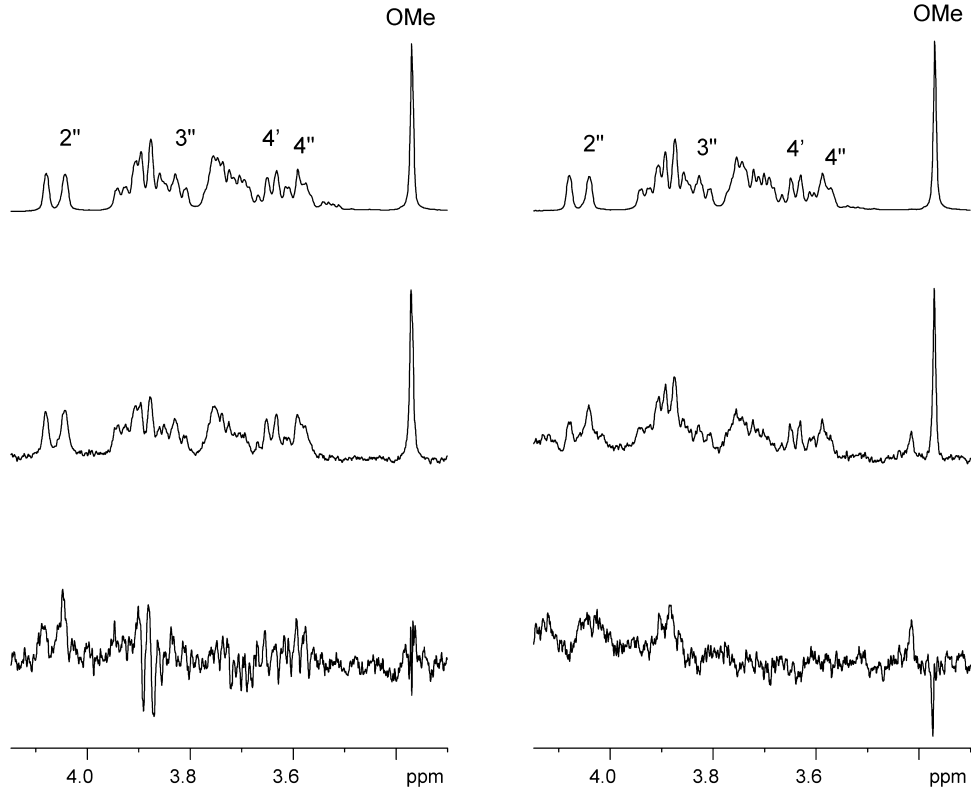

FIGURE 2: 1D ^{1}H NMR spectra of trisaccharide m2m2m, **4**, at 600 MHz and 10 °C in the presence of CV-N^{mutDA} (left) and CV-N^{mutDB} (right). Reference NMR spectra (top), STD NMR spectra (middle), and corrected STD NMR spectra obtained by subtracting the ligand-only STD NMR spectra from the spectrum obtained in the presence of protein (see Experimental Procedures).

effects were seen on the H2′, H3′, and H4′ signals, revealing these atoms as close contacts with the proteins. The very low intensity of the 6′-CH_3 signal in the STD NMR spectra indicates that the methyl group is remote from the binding pocket in the A domain.

STD signals were also observed with the 2′-deoxy derivative, **6**, indicating binding of this analogue to the proteins. The H3′ and H4′ resonances exhibited the largest effect, demonstrating their proximity to the protein. STD effects were also observed for H4 and H5 on the methyl mannoside

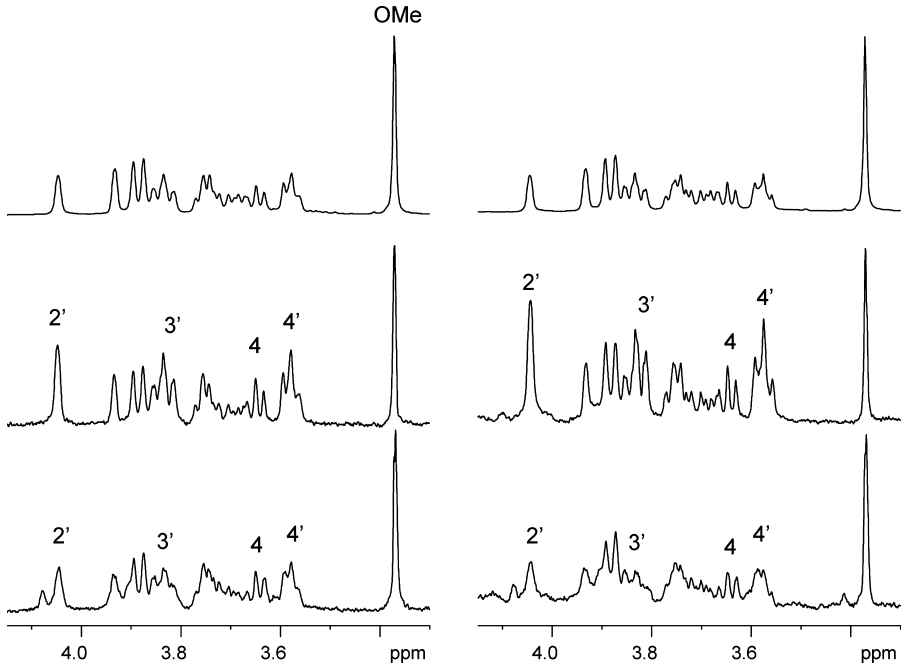

FIGURE 3: Competition STD NMR. Reference 1D proton spectrum of the of the weaker binding ligand m2m, **1**, in the presence of CV-N^{mutDA} (left) and CV-N^{mutDB} (right; top), the corresponding STD NMR spectra (middle), and spectra after addition of m2m2m, **4** (bottom).

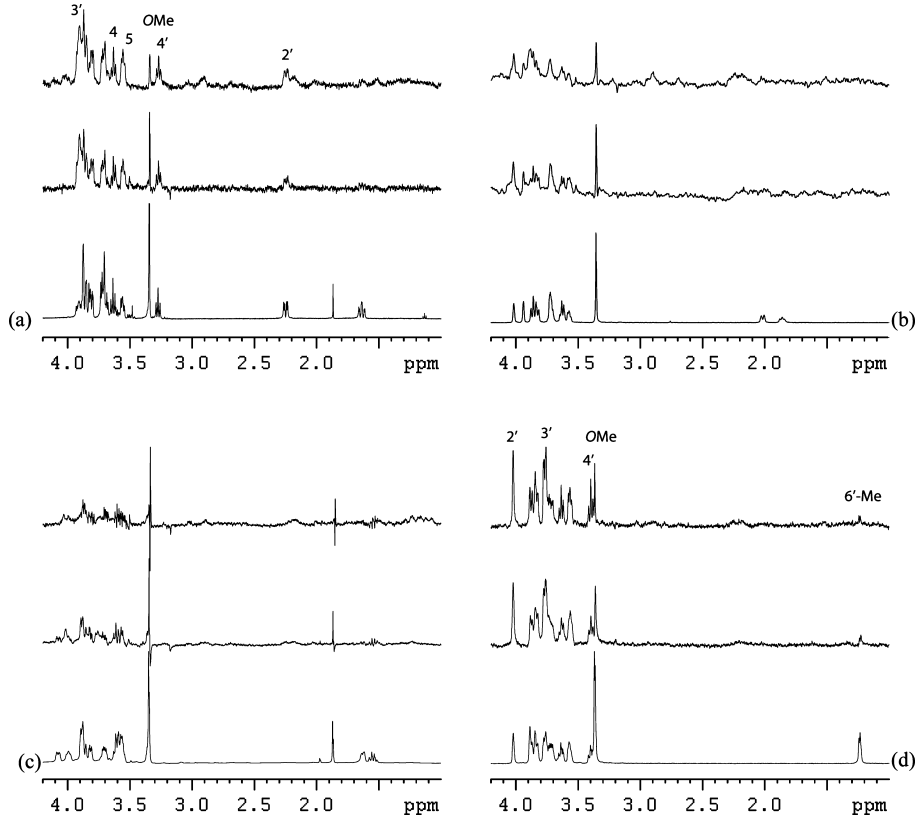

FIGURE 4: Reference (bottom spectra) and STD NMR spectra of (a) 2′-deoxy (**6**), (b) 3′-deoxy (**7**), (c) 4′-deoxy (**8**), and (d) 6′-deoxy (**9**) dimannosides in the presence of CV-N^{mutDA} (middle spectra) and CV-N^{mutDB} (top spectra).

residue. It is interesting to note that the axial proton at C-2 in the 2′-deoxy disaccharide, which replaces the hydroxyl group, does not give any signal in the STD NMR spectrum, suggesting that this proton is located away from the protein binding site. The equatorial H2 exhibits some STD effect, but to a much smaller degree compared to that of the parent compound carrying the 2′-axial hydroxyl group. This implies a less intimate interaction between the 2′-deoxy disaccharide and the protein. The 3′- and 4′-deoxy derivatives, **7** and **8**, respectively, caused only very weak residual signals in the STD NMR spectra, suggesting that these compounds do not bind to the protein. Competition STD NMR experiments using the 6′-deoxy disaccharide **9** as the weak binding ligand confirmed that the absence of STD signals was due to a lack

of binding rather than tight binding. Therefore, all the STD NMR experiments show that the C3′ and C4′ hydroxyl groups on the nonreducing end sugar are critical for binding to CV-N variants, whereas the C2′ and C6′ hydroxyl groups on the same sugar are nonessential.

The fact that there is no contact between the 6′-methyl group in the 6-deoxy disaccharide and the protein, as illustrated by the very weak STD effect, is in good agreement with the results obtained from experiments performed with the disaccharide Manα(1–2)Manα*O*Me, **1**, which did not show strong STD to the H6 protons. This is also in good agreement with the results from chemical shift mapping experiments that indicate stronger binding of the 6′-deoxy than the 2′-deoxy derivative vide infra.

Since the 3′- and 4′-hydroxyl groups on the nonreducing end sugar appeared to be required for binding, it was of interest to assess the importance of the hydroxyl group configuration at these two carbons. STD NMR experiments performed with the disaccharide α-D-Fuc(1–2)-D-Man in the presence of CV-N^{mutDB} gave no signals in the spectra, indicating that this disaccharide did not bind (data not shown). Compared to α-D-mannose, α-D-fucose has a 6-CH_3 group, an equatorial C2-OH group, and an axial C4-OH group. Since the 6′-deoxy dimannoside **9** and the 2′-deoxy compound bind to CV-N^{mutDB}, we are confident that an axial 2′-OH group is not required for the interaction. Therefore, the lack of binding of α-D-Fuc(1–2)-D-Man indicates that the configuration of the hydroxyl group at C4 is crucial. However, since the equatorial C2′-H group of mannose shows STD effects, the equatorial position of the hydroxyl group at C2 in fucose compared to its axial configuration in mannose may also play a role.

Chemical Shift Mapping Experiments. Chemical shift mapping is a powerful method for investigating protein–ligand interactions since it allows easy and quick identification of putative sites of interaction on the protein surface via detection of chemical shift perturbations in the $^1H-^{15}N$ HSQC spectrum of a uniformly labeled protein as a function of added (unlabeled) ligand. The $^1H-^{15}N$ HSQC spectra of uncomplexed CV-N mutants and of CV-N mutants in the presence of 15 molar equiv of 2′-deoxy dimannoside, **6**, are shown in Figure 5. A distinct set of perturbed amide N-H chemical shifts is observed, comprising nine residues in CV-N^{mutDA} and 15 residues in CV-N^{mutDB}. The affected residues are T7, G45, L47, Q50, N53, T57, G96, L98, and E101 for CV-N^{mutDA} and G2, K3, F4, S5, Q6, T7, C8, R24, T25, N26, N93, I94, G96, T97, and L98 for CV-N^{mutDB}. Addition of the 6′-deoxy dimannoside, **9**, perturbs the identical set of residues in CV-N^{mutDA} as seen with the 2′-deoxy disaccharide, whereas for CV-N^{mutDB}, four additional residues, G27, G28, Y29, and D95, are perturbed by the 6′-deoxy disaccharide (Figure 5).

A comparison of the $^1H-^{15}N$ correlation spectra of the mutants in the presence of the 2′- and 6′-deoxy compounds revealed some differences. Spectra for complexes of CV-N^{mutDA} with 2′-deoxy and 6′-deoxy dimannoside were nearly identical, while in spectra for complexes of CV-N^{mutDB}, the differences in chemical shifts upon interaction were slightly larger for the 6′-deoxy dimannoside. In particular, the K3, I94, and D95 resonances exhibited this trend. It can be noted that titration of CV-N^{mutDB} and CV-N^{mutDA} with the 6-deoxy compound resulted in similar shifts as previously observed

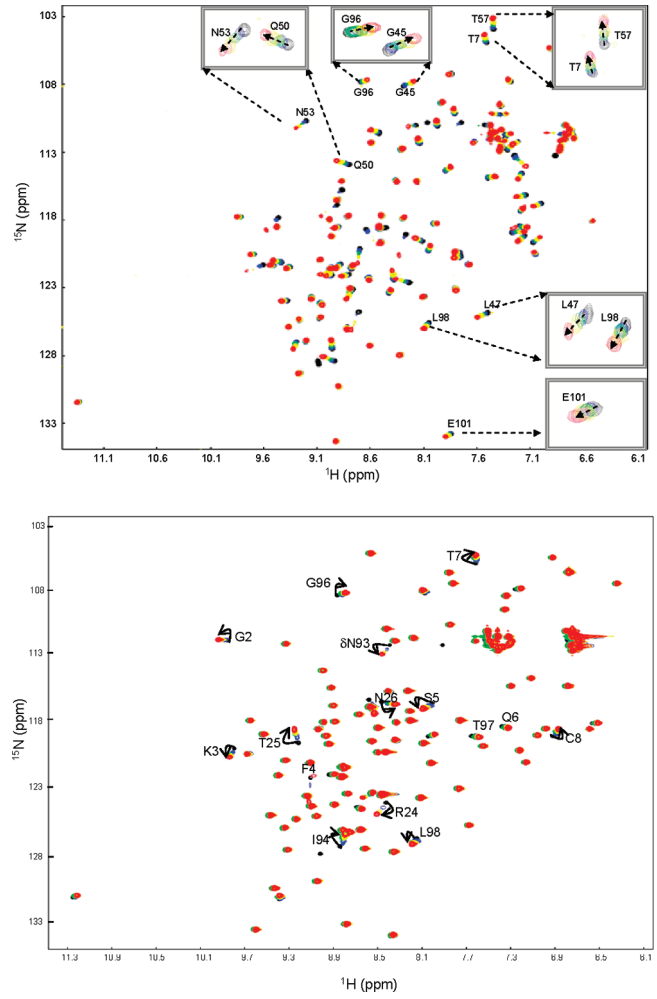

FIGURE 5: Superposition of the $^1H-^{15}N$ HSQC NMR spectra of CV-N^{mutDA} (top) and CV-N^{mutDB} (bottom) free and in the presence of 2′-deoxy dimannoside **6**. The spectra without and with 15 molar equiv of **6** are colored black and red, respectively. The resonances that shift upon addition of the disaccharide are labeled with residue name and number, and selected signals are shown in an expanded view (boxed).

with Man-9, m2m2m, and m2m (*25*) in their $^1H-^{15}N$ HSQC NMR spectra. This indicates similar binding behavior for the interaction with the binding site on domain A^M (wild-type CV-N and CV-N^{mutDB}) and on domain B^M (wild-type and CV-N^{mutDA}). The fact that G27, G28, Y29, and D95 in CV-N^{mutDB} were affected by the presence of the 6′-deoxy but not by the 2′-deoxy disaccharide suggests that these amino acid residues interact with the C2′ hydroxyl group in the sugar.

The $^1H-^{15}N$ HSQC NMR spectra of the two mutants in the presence of 3′-deoxy or 4′-deoxy dimannosides **7** and **8**, respectively, were unchanged from those of the proteins alone (Figure 6 of the Supporting Information), indicating that no interaction occurs.

DISCUSSION

The overall goal in the design of the two mutant CV-N forms was to create a protein that preserved the overall wild-type CV-N fold, with one of the two binding sites removed (CV-N^{mutDB}) or with altered specificity of one of the sites (CV-N^{mutDA}). The design and biophysical characterization of the two mutant proteins were reported in ref (*25*). Structural

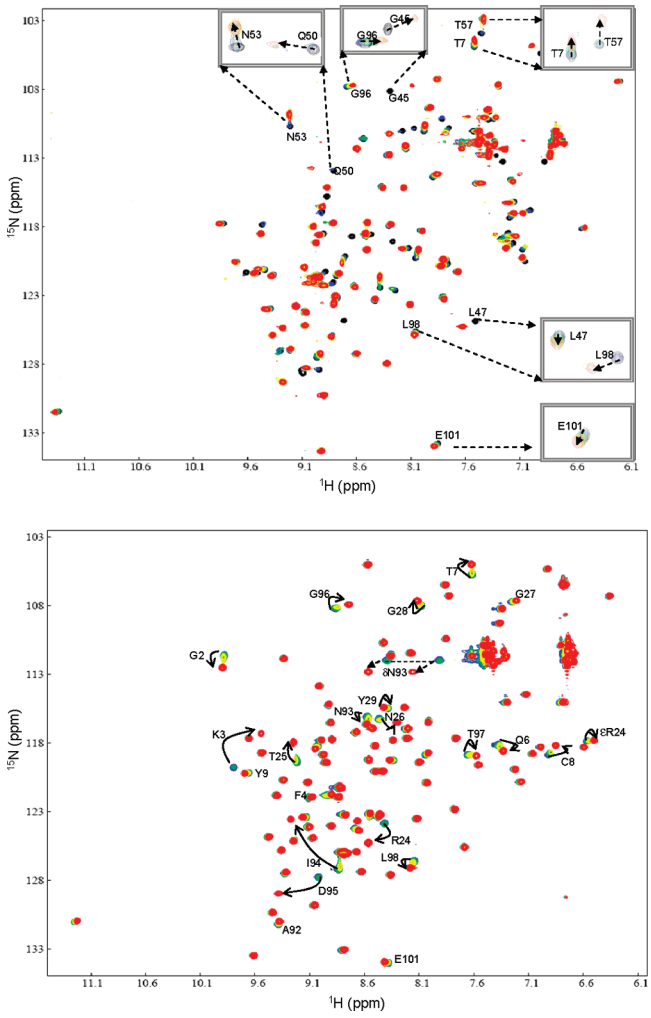

FIGURE 6: Superposition of the ^{1}H−^{15}N HSQC NMR spectra of CV-N^{mutDA} (top) and CV-N^{mutDB} (bottom) free and in the presence of the 6′-deoxy dimannoside **9**. The spectra without and with 15 molar equiv of **9** are colored black and red, respectively. The resonances that shift upon addition of the disaccharide are labeled with residue name and number, and selected signals are shown in an expanded view (boxed).

characterization of the two mutants was carried out by NMR spectroscopy, and for both proteins, the ^{1}H−^{15}N HSQC NMR spectra showed the characteristic distribution of resonances compatible with the wild-type CV-N fold. Indeed, backbone assignment validated that the overall structures of these mutants were very similar to that of native CV-N. In addition, multiangle light scattering and native gel electrophoresis confirmed that the proteins were monomeric. The thermal stabilities of the mutants were virtually identical to that of the parent monomeric P51GCV-N (*25*). The one binding site containing variant, CV-N^{mutDB}, is unique since it allowed us to directly investigate sugar binding without the complications that are inherent in binding studies of CV-N where sugar binding can occur to two sites simultaneously.

For the different oligosaccharides Manα(1–2)Manα*O*Me, Manα(1–2)Manα(1–3)Manα*O*Me, and Manα(1–2)Manα(1–6)Manα*O*Me, the strongest STD signals were observed for H2, H3, and H4 on the terminal sugar at the nonreducing end, positioning it in close contact with the protein. In addition, the H4 signal of the penultimate sugar residue also experienced strong STD effects. Since very similar results were obtained for both mutants, similar binding modes for the terminal nonreducing end in the two different sites can be assumed. We also established that the Manα(1–2)Manα(1–2)Manα*O*Me trisaccharide, **4**, exhibited the highest affinity for both mutants.

These results with the designed mutants of CV-N confirm and extend results obtained previously with the wild-type protein which showed that not only the terminal disaccharide but also the neighboring mannose residue influences the affinity and selectivity of the interaction (*24*). Most likely, the conformation of the glycosidic linkage between the common terminal disaccharide and the original reducing mannopyranose ring is responsible for the observed selectivity. Indeed, the presence of two 1,2-glycosidic linkages in Manα(1–2)Manα(1–2)Manα*O*Me, **4**, leads to a structure more compact than that of Manα(1–2)Manα(1–3)Manα*O*Me, **2**, and Manα(1–2)Manα(1–6)Manα*O*Me, **3**, with the 1,3- and 1,6-glycosidic linkages, allowing a larger degree of conformational variability.

In the carbohydrate binding site in the B domain of wild-type CV-N, the hydroxyl groups of both sugars of the disaccharide m2m interact with the side chains of polar and charged residues Glu41, Ser52, Glu56, and Thr57 and Asp44, Lys74, Thr75, Arg76, and Gln78, respectively (*12, 14*). In the CV-N^{mutDB} mutant, four of these key polar residues in domain B, Glu41, Asn42, Thr57, and Arg76, were replaced with nonpolar Ala residues. Therefore, this mutant protein is no longer capable of binding to any mannose oligosaccharide. The STD NMR experiments confirm that the remaining binding site in the A domain is still able to bind carbohydrates. As anticipated, Manα(1–2)Manα(1–2)Manα*O*Me trisaccharide **4** interacts most strongly with CV-N^{mutDB} in the site on domain A (K_d ∼ 4 μM), while Manα(1–2)Manα*O*Me disaccharide **1** and Manα(1–2)Manα(1–3)Manα*O*Me **2** and Manα(1–2)Manα(1–6)Manα*O*Me **3** bind with a lower affinity [K_d ∼ 750 μM for Manα(1–2)Manα].

In the sugar binding site of domain A, many of the hydroxyls of the disaccharide Manα(1–2)Man were proposed to form direct or water-mediated hydrogen bonds with Lys3, Gln6, Thr7, Glu23, Thr25, and Asn93 (*12*). Four of these six residues were replaced with amino acids whose side chains lacked hydrogen bond donors or acceptors or were too short to engage in contacts with Manα(1–2)Man. Several additional amino acid changes were also introduced to prevent unfavorable steric interactions. Therefore, in the CV-N^{mutDA} mutant comprising the Lys3Asn, Gln6Glu, Glu23Cys, Arg24Thr, Thr25Arg, Asn26Ala, Gly27Leu, Gly28Gln, Pro51Gly, and Ala92Glu changes, the binding site on domain A is more similar to that on domain B. In this way, the preference for trimannoside Manα(1–2)Manα(1–2)Manα*O*Me **4** was expected to be eliminated, while the ability to recognize the Manα(1–2)Man epitope should be retained. The STD NMR results reveal that indeed CV-N^{mutDA} recognizes the terminal nonreducing end of Manα(1–2)Manα*O*Me, **1**, Manα(1–2)Manα(1–3)Manα*O*Me, **2**, and Manα(1–2)Manα(1–6)Manα*O*Me, **3**, equally well as Manα(1–2)Manα(1–2)Manα*O*Me, **4**.

Hydrogen bonds to hydroxyl groups of sugars are thought to play a key role in the carbohydrate recognition process. Thus, having established that H2, H3, and H4 on the nonreducing mannopyranose experienced the largest saturation transfer and thus are in closest contact with the protein,

Scheme 3: Reagents and Conditions for Synthesis of Monodeoxy Disaccharides **6–9**

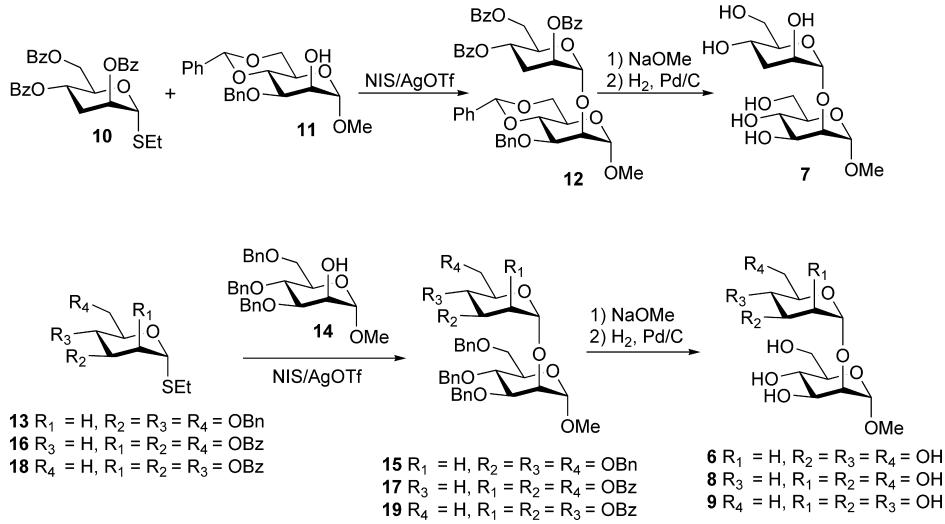

we performed NMR binding studies with the corresponding deoxy sugar derivatives to investigate whether all hydroxyls or a subset were critical for the hydrogen bonding interactions.

The results of the STD NMR experiments using deoxy analogues **6**−**9** of disaccharide Manα(1–2)Man*O*Me **1** demonstrated that the 3′- and 4′-hydroxyl groups of the nonreducing mannopyranose moiety are the key polar groups required for recognition by the CV-N proteins, with the 2′- and 6′-hydroxyls playing a minor role. Clearly, under equivalent conditions, the 2′- and 6′-deoxy compounds bind, whereas the 3′- and 4′-deoxy derivatives do not. In the crystal structure of the hexamannoside−CV-N complex (*14*) where Manα(1–2)Man is the binding element, O3 and O4 of the reducing and nonreducing end are involved in five and four hydrogen bonds with the protein, respectively. The lengths of the hydrogen bonds with the terminal nonreducing end are slightly shorter that those for the reducing end. These data are in good agreement with our NMR results that show that 3′- and 4′-hydroxyl groups on the terminal nonreducing end sugar are required for binding. In addition to the polar interactions, the noted strong STD effects observed for H2′ in Manα(1–2)Man*O*Me **1** may implicate a nonpolar contact between the proton at the 2′ position and the protein. Since the C2 atom plays a pivotal role in the 1,2-linkage of the dimannoside, the configuration at C2 is also a determinant in sugar binding, allowing the molecule to adopt a compact conformation with the two sugars stacked on top of each other. Therefore, the optimal combination of conformation and the availability of the correct hydroxyl groups are clearly important for dimannoside binding to CV-N and most likely for all sugar−protein interactions.

EXPERIMENTAL PROCEDURES

Compounds **1**−**5** were available from previous studies (*24*), and the expression and purification of the two mutant proteins, CV-N^{mutDA} and CV-N^{mutDB}, have been reported previously (*25*).

*Synthesis of Deoxy Sugars **6–9.*** The deoxy disaccharides **6**−**9** were synthesized in a manner similar to that described for other mannose deoxy di- and trisaccharides (*27, 28*). Thus, the deoxy function was introduced at the monosaccharide level, and the deoxy derivatives were transformed into the ethyl thioglycoside donors **10**, **13**, **16**, and **18**, which were used in NIS/AgOTf-promoted couplings with either of the two 2-OH acceptors **11** and **14** to give protected disaccharides **12**, **15**, **17**, and **19**, respectively (Scheme 3). Deprotection, methoxide treatment to remove benzoyl esters, and catalytic hydrogenolysis to remove benzyl ethers and benzylidene acetals then afforded the target structures **6**−**9**. The ^{1}H NMR chemical shifts for **6–9** in D_2O are reported in Table 1.

Methyl 3-Deoxy-α-D-arabino-hexopyranosyl(1→2)-α-D-mannopyranoside (7). A mixture of methyl 3-*O*-benzyl-4,6-*O*-benzylidene-α-D-mannopyranoside (*29*) (**11**, 66 mg, 0.18 mmol) and ethyl 2,4,6-tri-*O*-benzoyl-3-deoxy-1-thio-α-D-*arabino*-hexopyranoside (**10**, 62 mg, 0.12 mmol) in dry CH_2Cl_2 (5 mL) containing powdered 4 Å molecular sieves was stirred under N_2 at 0 °C for 15 min. NIS (41 mg, 0.18 mmol) and AgOTf (catalytic amount) were added successively, and the reaction mixture was stirred at 0 °C for 40 min and thereafter neutralized by dropwise addition of Et_3N. Methyl 2,4,6-tri-*O*-benzoyl-3-deoxy-α-D-*arabino*-hexopyranosyl(1→2)-3-*O*-benzyl-4,6-*O*-benzyliden-α-D-mannopyranoside (**12**, 49 mg, 50%) was obtained after purification by silica gel flash chromatography (toluene/EtOAc, 12.5:1). Compound **12** (49 mg, 0.06 mmol) was dissolved in MeOH (3 mL) and treated with NaOMe (0.2 mL, 1 M). After being stirred for 2 h at room temperature, the reaction mixture was neutralized using DOWEX 50 (H^+) ion-exchange resin, filtered, concentrated, and purified by silica gel flash chromatography (CH_2Cl_2/MeOH, 12.5:1) to give disaccharide methyl 3-deoxy-α-D-*arabino*-hexopyranosyl(1→3)-3-*O*-benzyl-4,6-*O*-benzyliden-α-D-mannopyranoside (14 mg, 47%). This compound (10 mg, 0.02 mmol) was dissolved in dry MeOH (2 mL), and a catalytic amount of Pd/C was added. The reaction mixture was stirred under H_2 gas for 12 h. The catalyst was removed by filtration, and the solvent evaporated under reduced pressure. Purification of the residue on a 600 mg C18 MAXI-CLEAN cartridge (Alltech, eluted with H_2O) afforded **7** (7 mg, 98%).

Methyl 2-Deoxy-α-D-arabino-hexopyranosyl(1→2)-α-D-mannopyranoside (6). EtSH (65 μL, 1.2 mmol) was added in portions to a cooled (0 °C) solution of 3,4,6-tri-*O*-benzyl-D-glucal (100 mg, 0.24 mmol) and CAN (13.2 mg, 0.024

Table 1: ^{1}H and ^{13}C NMR Chemical Shifts (parts per million) at 10 °C of the 2′-, 3′-, 4′-, and 6′-Deoxy Analogues **6–9** of Manα(1–2)-Manα*O*Me

	H1	H2	H3	H4	H5	H6	OMe
2′-deoxy-Manα(1–2)Manα*O*Me (**6**)	5.129	1.638/2.248	3.913	3.275	3.712	3.700/3.837	
	99.9	36.8	68.0	71.2	72.8	60.9	
	4.923	3.872	3.815	3.636	3.563	3.719/3.808	3.344
	99.4	77.9	70.4	67.0	72.5	61.0	54.8
3′-deoxy-Manα(1–2)Manα*O*Me (**7**)	4.814	4.01	1.862/2.018	3.720	3.700	3.622/3.850	
	1009.9	67.1	33.2	61.6	74.1	61.2	
	5.006	3.938	3.817	3.615	3.571	3.724/3.868	3.355
	99.4	78.0	70.3	67.0	72.5	60.9	54.8
4′-deoxy-Manα(1–2)Manα*O*Me (**8**)	5.007	3.879	4.076	1.545/1.625	3.995	3.565/3.602	
	103.0	67.9	64.8	28.7	69.8	64.1	
	4.951	3.895	3.814	3.601	3.547	3.704/3.864	3.348
	99.5	78.2	70.2	67.0	72.6	60.9	54.8
6′-deoxy-Manα(1–2)Manα*O*Me (**9**)	4.918	4.021	3.770	3.399	3.757	1.238	
	102.1	70.0	70.0	72.0	69.0	16.6	
	4.823	3.886	3.827	3.638	3.571	3.717/3.854	3.366
	99.5	78.1	70.2	66.9	72.7	60.8	54.8

mmol) in MeCN (3 mL). The reaction mixture was stirred at room temperature for 2 days and then purified by flash chromatography (toluene/EtOAc, 50:1) to give ethyl 3,4,6-tri-*O*-benzyl-2-deoxy-1-thio-α/β-D-*arabino*-hexopyranoside (**13**, 90 mg, 79%). Donor **13** (175 mg, 0.36 mmol) and methyl 3,4,6-tri-*O*-benzyl-α-D-mannopyranoside (*28*) (**14**, 295 mg, 0.63 mmol) were dissolved in CH_2Cl_2 (5 mL) followed by addition of molecular sieves. The reaction mixture was stirred at 0 °C for 15 min, after which NIS (145 mg, 0.63 mmol) and AgOTf (catalytic amount) were added and the reaction mixture was stirred for an additional 5 min, then concentrated, and purified by silica gel flash chromatography (toluene/EtOAc, 12.5:1) to yield methyl 3,4,6-tri-*O*-benzyl-2-deoxy-α-D-*arabino*-hexopyranosyl(1→2)-3,4,6-tri-*O*-benzyl-α-D-mannopyranoside (**15**, 81 mg, 34%). A mixture of disaccharide **15** (42 mg, 0.048 mmol) and a catalytic amount of Pd/C (10%) in THF, MeOH, and water (2 mL, 2 mL, and 50 μL, respectively) was stirred under hydrogen at room temperature for 12 h. Purification on a 600 mg C18 MAXI-CLEAN cartridge (as described above) afforded **6** (8 mg, 52%).

*Methyl 4-Deoxy-*α*-D-lyxo-hexopyranosyl(1→2)-*α*-D-mannopyranoside (**8**).* Acceptor **14** (61 mg, 0.13 mmol) and ethyl 2,3,6-tri-*O*-benzoyl-4-deoxy-1-thio-α-D-*lyxo*-hexopyranoside (**16**, 46 mg, 0.09 mmol) in dry CH_2Cl_2 (5 mL) were coupled as described above for the synthesis of compounds **7** and **15** to yield methyl 2,3,6-tri-*O*-benzoyl-4-deoxy-α-D-*lyxo*-hexopyranosyl (1→2)-3,4,6-tri-*O*-benzyl-α-D-mannopyranoside (**17**, 47 mg, 62%). Compound **17** (47 mg, 0.05 mmol) was deprotected as described for compound **12** above to afford **8** (9 mg, 53%).

*Methyl 6-Deoxy-*α*-D-mannopyranosyl(1→2)-*α*-D-mannopyranoside (**9**).* Acceptor **14** (79 mg, 0.15 mmol) and methyl 2,3,4-tri-*O*-benzoyl-6-deoxy-1-thio-α-D-mannopyranoside (**18**, 59 mg, 0.11 mmol) were coupled as described above for the synthesis of compounds **12** and **15** to afford methyl 2,3,4-tri-*O*-benzoyl-6-deoxy-α-D-mannopyranosyl-(1→2)-3,4,6-tri-*O*-benzyl-α-D-mannopyranoside (**19**, 66 mg, 65%). Compound **14** (47 mg, 0.05 mmol) was deprotected as described for compound **12** above to afford **9** (21 mg, 76%).

STD NMR Experiments. All STD NMR experiments were carried out on a Bruker DRX-600 spectrometer using a 2.5 mm selective $^{1}H/^{13}C$ microprobe equipped with a z gradient. The Bruker software XWIN-NMR was used for data acquisition and processing. Each NMR sample contained 78 μM $CV\text{-}N^{mutDA}$ or $CV\text{-}N^{mutDB}$ mutant protein and a 100-fold excess of ligand **1**, **2**, **3**, **4**, or **5** or a 50-fold excess of ligand **6**, **7**, **8**, or **9** in 20 mM phosphate buffer (pH 6.0), 0.05% NaN_3, and 99.96% D_2O.

NMR spectra were recorded at 10 and 25 °C with the residual HDO signal used as an internal reference (δ 4.94 at 10 °C and δ 4.74 at 25 °C). The one-dimensional proton reference and STD NMR spectra were recorded using WATERGATE (*30*) for water suppression. The STD and reference NMR spectra were acquired with 2048 scans, and FIDs were multiplied by an exponential line broadening function of 1 Hz prior to Fourier transformation. The selective saturation of the protein was achieved using a pulse train of 40 Gaussian-shaped pulses with a duration of 50 ms, each separated by a 1 ms delay.

Since the size of the CV-N mutants (∼11 kDa) is close to the limit of 10 kDa, suggested to be the smallest size for which effective saturation of the entire protein by spin diffusion can be achieved and rendering it suitable for STD NMR experiments (*23*), it was necessary to ensure that efficient magnetization transfer occurred. For large proteins, on-resonance saturation is usually set to values around δ −1. In CV-N, no protein proton resonates around δ −1 and relatively narrow lines are present. It was therefore necessary to set the saturation frequencies directly on or very close to protons signals from the protein and ascertain that the STD signal enhancements were not due to a direct saturation transfer from specific protein protons to the sugar. To evaluate this possibility and rule out direct transfer, we used several saturation frequencies. Evaluating the saturation frequency dependence of the STD NMR spectra for protein/m2m samples revealed that for a saturation time of 2 s, very similar STD spectra were obtained. This confirmed that full saturation of the protein by spin diffusion was achieved. A saturation time of 1 s, however, was insufficient for efficient transfer of saturation from the protein to the ligand protons when the saturation frequency was set at δ 0.25 and 7. This was most likely due to the lower protein proton density at these frequencies resulting in suboptimal saturation of all of the protein resonances. All subsequent STD NMR spectra for **1–5** were therefore recorded with the saturation frequency set at δ 0.4, since this region contains most methyl resonances of the protein and irradiation at protein methyls has previously been found to yield the most effective

saturation (*31*). In addition, it should be pointed out that this frequency is far from the *O*Me signal of the sugars, ensuring that no perturbation of this sugar resonance can be induced by the selective shaped pulse. For compounds **6–9**, the saturation frequency was set at δ 7.0 since the deoxy protons of the sugars were also affected with irradiation at δ 0.4.

We recorded all STD NMR spectra at 10 °C since in preliminary experiments on CV-N/m2m samples (*24*) we noted that higher STD-NMR intensities were observed at this temperature than at 25 °C. The enhancement patterns, on the other hand, are however very similar at 10 and 25 °C, with maximum enhancements for the H2, H3, and H4 signals of the nonreducing end of m2m. The same observations hold for experiments with trisaccharides **2–4**. In this work, we carried out the equivalent experiments with the mutants and again observed that similar relative STD enhancements are seen, while the STD-NMR intensities are higher at 10 °C than at 25 °C. It has previously been suggested (*31*) that the predominant factor leading to larger STD enhancements at lower temperatures is the slower molecular tumbling of the molecule. The slower tumbling of the protein accelerates the spread of saturation over the entire protein and, in turn, the transfer of saturation to the bound ligand. This temperature effect was shown to be more important for small proteins. At 4 °C, a saturation time of 1.5 s was necessary to saturate all resonances of the 22 kDa protein DHFR, while a 3-fold longer time (4.5 s) was required at 30 °C (*31*). Low-temperature-induced enhancements of STD signal intensities have also been reported in other studies (*32, 33*).

To investigate the dependence of the STD NMR spectra of CV-N/m2m, **1**, on the saturation time, STD NMR spectra for **1** were obtained with saturation times ranging from 0.5 to 6 s, incremented in 1 s steps. Two seconds was sufficient for efficient transfer of saturation from the protein to the sugar protons, and for 2 s or more, similar STD spectra were obtained, with maximum enhancements for H2, H3, and H4 of the nonreducing end of the sugar. With a saturation time of 1 s, enhancement of H2, H3, and H4 of the terminal unit was also observed, but the signal-to-noise ratio was lower. A saturation time of 0.5 s was too short. Since the small size of the protein leads to slow spin diffusion rates and a reduced level of saturation transfer to the ligand, longer times are necessary for the magnetization to spread out (*34*).

The reference STD spectra were recorded with the off-resonance frequency set at δ 30. The saturated spectra were subtracted from the reference spectra via phase cycling. Control STD experiments recorded with ON and OFF saturation frequencies set to identical values (δ 0.4 or 30) were also recorded. The resulting difference spectra were devoid of any signals, proving that good subtraction was achieved.

In addition, samples containing only the carbohydrate ligands at the same concentration as the one used in the presence of the proteins were subjected to STD NMR experiments with the on-resonance set at δ 0.4 or 7.0 and the off-resonance at δ 30 using a saturation time of 4 s. For the high ligand concentration used for **1–5**, the resulting difference spectra contained small amounts of the normal 1D NMR spectra. These effects of free ligand were corrected by subtracting the STD NMR spectrum obtained for the ligand/protein mixture from the one obtained for the ligand alone. With the lower ligand concentration used with **6–9**, the STD spectra showed no residual NMR signals. Such spurious residual signals have been previously observed at higher ligand concentrations (*35*).

The ^{1}H spin–lattice relaxation times were measured using an inversion–recovery experiment (*36*).

NMR Sugar Titration Experiments. Titration experiments with 2′-deoxy, 3′-deoxy, 4′-deoxy, and 6′-deoxy m2m were performed using ^{15}N-labeled protein samples (75 μM CV-N^{mutDA} and 150 μM CV-N^{mutDB}) in 20 mM sodium phosphate buffer (pH 6.0), 0.01% sodium azide, and a 90% H_2O/10% D_2O mixture at 30 °C. A series of ^{1}H−^{15}N HSQC spectra were recorded after addition of sugar aliquots from stock solutions of 3.9 mM synthetic 2′-deoxy, 4.5 mM 3′-deoxy, 4.7 mM 4′-deoxy, and 5 mM 6′-deoxy sugars. The concentrations of the synthetic oligosaccharides were determined by compositional analysis performed by the Complex Carbohydrate Research Center of the University of Georgia (Athens, GA). ^{1}H−^{15}N HSQC spectra were recorded using a Bruker DRX-600 spectrometer, equipped with a *z*-axis gradient cryoprobe. Spectra were processed with NMRPipe and analyzed using NMRDraw and NMRView.

SUPPORTING INFORMATION AVAILABLE

1D STD NMR spectra of Manα(1–2)Manα(1–3)Manα-*O*Me, Manα(1–2)Manα(1–6)Manα*O*Me, and Manα(1–3)-[Manα1–6]Manα*O*Me in the presence of CV-N^{mutDA} and CV-N^{mutDB} at 10 °C, competition STD NMR spectra for Manα(1–3)[Manα1–6]Manα*O*Me, and ^{1}H−^{15}N HSQC NMR spectra of CV-N^{mutDA} and CV-N^{mutDB} free and in the presence of 3′- and 4′-deoxydimannosides. This material is available free of charge via the Internet at http://pubs.acs.org.

REFERENCES

1. Boyd, M. R., Gustafson, K. R., McMahon, J. B., Shoemaker, R. H., Okeefe, B. R., Mori, T., Gulakowski, R. J., Wu, L., Rivera, M. I., Laurencot, C. M., Currens, M. J., Cardellina, J. H., Buckheit, R. W., Nara, P. L., Pannell, L. K., Sowder, R. C., and Henderson, L. E. (1997) Discovery of Cyanovirin-N, a novel human immunodeficiency virus-inactivating protein that binds viral surface envelope glycoprotein gp120: Potential applications to microbicide development. *Antimicrob. Agents Chemother. 41*, 1521–1530.
2. Esser, M. T., Mori, T., Mondor, I., Sattentau, Q. J., Dey, B., Berger, E. A., Boyd, M. R., and Lifson, J. D. (1999) Cyanovirin-N binds to gp120 to interfere with CD4-dependent human immunodeficiency virus type 1 virion binding, fusion, and infectivity but does not affect the CD4 binding site on gp120 or soluble CD4-induced conformational changes in gp120. *J. Virol. 73*, 4360–4371.
3. Dey, B., Lerner, D. L., Lusso, P., Boyd, M. R., Elder, J. H., and Berger, E. A. (2000) Multiple antiviral activities of Cyanovirin-N: Blocking of human immunodeficiency virus type 1 gp120 interaction with CD4 and coreceptor and inhibition of diverse enveloped viruses. *J. Virol. 74*, 4562–4569.
4. Barrientos, L. G., O'Keefe, B. R., Bray, M., Anthony, S., Gronenborn, A. M., and Boyd, M. R. (2003) Cyanovirin-N binds to the viral surface glycoprotein, $GP_{1,2}$ and inhibits infectivity of Ebola virus. *Antiviral Res. 58*, 47–56.
5. O'Keefe, B. R., Smee, D. F., Turpin, J. A., Saucedo, C. J., Gustafson, K. R., Mori, T., Blakeslee, D., Buckheit, R., and Boyd, M. R. (2003) Potent anti-influenza activity of Cyanovirin-N and interactions with viral hemagglutinin. *Antimicrob. Agents Chemother. 47*, 2518–2525.
6. Barrientos, L. G., and Gronenborn, A. M. (2005) The highly specific carbohydrate-binding protein Cyanovirin-N: Structure, anti-HIV/Ebola activity and possibilities for therapy. *Rev. Med. Chem. 5*, 21–31.
7. O'Keefe, B. R., Shenoy, S. R., Xie, D., Zhang, W. T., Muschik, J. M., Currens, M. J., Chaiken, I., and Boyd, M. R. (2000) Analysis

of the interaction between the HIV-inactivating protein Cyanovirin-N and soluble forms of the envelope glycoproteins gp120 and gp41. *Mol. Pharmacol. 58*, 982–992.

8. Bolmstedt, A. J., O'Keefe, B. R., Shenoy, S. R., McMahon, J. B., and Boyd, M. R. (2001) Cyanovirin-N defines a new class of antiviral agent targeting N-linked, high-mannose glycans in an oligosaccharide-specific manner. *Mol. Pharmacol. 59*, 949–954.
9. Shenoy, S. R., O'Keefe, B. R., Bolmstedt, A. J., Cartner, L. K., and Boyd, M. R. (2001) Selective interactions of the human immunodeficiency virus-inactivating protein cyanovirin-N with high-mannose oligosaccharides on gp120 and other glycoproteins. *J. Pharmacol. Exp. Ther. 297*, 704–710.
10. Bewley, C. A., Gustafson, K. R., Boyd, M. R., Covell, D. G., Bax, A., Clore, G. M., and Gronenborn, A. M. (1998) Solution structure of cyanovirin-N, a potent HIV-inactivating protein. *Nat. Struct. Biol. 5*, 571–578.
11. Yang, F., Bewley, C. A., Louis, J. M., Gustafson, K. R., Boyd, M. R., Gronenborn, A. M., Clore, G. M., and Wlodawer, A. (1999) Crystal structure of cyanovirin-N, a potent HIV-inactivating protein, shows unexpected domain swapping. *J. Mol. Biol. 288*, 403–412.
12. Bewley, C. A. (2001) Solution structure of a Cyanovirin-N:Manα1–2Manα complex: Structural basis for high-affinity carbohydrate-mediated binding to gp120. *Structure 9*, 931–940.
13. Barrientos, L. G., Louis, J. M., Botos, I., Mori, T., Han, Z. Z., O'Keefe, B. R., Boyd, M. R., Wlodawer, A., and Gronenborn, A. M. (2002) The domain-swapped dimer of Cyanovirin-N is in a metastable folded state: Reconcilition of X-ray and NMR structures. *Structure 10*, 673–686.
14. Botos, I., O'Keefe, B. R., Shenoy, S. R., Cartner, L. K., Ratner, D. M., Seeberger, P. H., Boyd, M. R., and Wlodawer, A. (2002) Structures of the complexes of a potent anti-HIV protein Cyanovirin-N and high mannose oligosaccharides. *J. Biol. Chem. 277*, 34336–34342.
15. Barrientos, L. G., Louis, J. M., Ratner, D. M., Seeberger, P. H., and Gronenborn, A. M. (2003) Solution structure of a circular-permuted variant of the potent HIV-inactivating protein Cyanovirin-N: Structural basis for protein stability and oligosaccharide interaction. *J. Mol. Biol. 325*, 211–223.
16. Bewley, C. A., and Otero-Quintero, S. (2001) The potent anti-HIV cyanovirin-N contains two novel carbohydrate binding sites that selectively bind to Man_8 D1D3 and Man_9 with nanomolar affinity: Implications for binding to the HIV envelope protein gp120. *J. Am. Chem. Soc. 123*, 3892–3902.
17. Shenoy, S. R., Barrientos, L. G., Ratner, D. M., O'Keefe, B. R., Seeberger, P. H., Gronenborn, A. M., and Boyd, M. R. (2002) Multisite and multivalent binding between Cyanovirin-N and branched oligomannosides: Calorimetric and NMR characterization. *Chem. Biol. 9*, 1109–1118.
18. Bewley, C. A., Kiyonaka, S., and Hamachi, I. (2002) Site-specific discrimination by Cyanovirin-N for α-linked trisaccharides comprising the three arms of Man_8 and Man_9. *J. Mol. Biol. 322*, 881–889.
19. Mayer, M., and Meyer, B. (1999) Characterization of ligand binding by saturation transfer difference NMR spectroscopy. *Angew. Chem., Int. Ed. 38*, 1784–1788.
20. Klein, J., Meinecke, R., Mayer, M., and Meyer, B. (1999) Detecting binding affinity to immobilized receptor proteins in compound libraries by HR-MAS STD NMR. *J. Am. Chem. Soc. 121*, 5336–5337.
21. Vogtherr, M., and Peters, T. (2000) Application of NMR based binding assays to identify key hydroxy groups for intermolecular recognition. *J. Am. Chem. Soc. 122*, 6093–6099.
22. Mayer, M., and Meyer, B. (2001) Group epitope mapping by saturation transfer difference NMR to identify segments of a ligand in direct contact with a protein receptor. *J. Am. Chem. Soc. 123*, 6108–6117.
23. Meyer, B., and Peters, T. (2003) NMR spectroscopy techniques for screening and identifying ligand binding to protein receptors. *Angew. Chem., Int. Ed. 42*, 864–890.
24. Sandström, C., Berteau, O., Gemma, E., Oscarson, S., Kenne, L., and Gronenborn, A. M. (2004) Atomic mapping of the interactions between the antiviral agent Cyanovirin-N and oligomannosides by saturation-transfer difference NMR. *Biochemistry 43*, 13926–13931.
25. Barrientos, L. G., Matei, E., Lasala, F., Delgado, R., and Gronenborn, A. M. (2006) Dissecting carbohydrate-Cyanovirin-N binding by structure-guided mutagenesis: Functional implications for viral entry inhibition. *Protein Eng., Des. Sel. 19*, 525–535.
26. Wang, Y. S., Liu, D. J., and Wyss, D. F. (2004) Competition STD NMR for the detection of high-affinity ligands and NMR-based screening. *Magn. Reson. Chem. 42*, 485–489.
27. Oscarson, S., and Tedebark, U. (1995) Synthesis of deoxy analogues of methyl 3,6-di-O-α-D-mannopyranosyl-α-D-mannopyranoside for studies of the binding site of Concanavalin A. *Carbohydr. Res. 278*, 271–287.
28. Gemma, E., Lahmann, M., and Oscarson, S. (2006) Synthesis of monodeoxy analogues of the trisaccharide α-D-Glcp-(1–3)-α-D-Manp-(1–2)-α-D-Manp*O*Me recognized by calreticuli/calnexin. *Carbohydr. Res. 341*, 1533–1542.
29. Boger, D. L., and Honda, T. (1994) Total synthesis of Bleomycin A2 and related agents. 4. Synthesis of the disaccharide subunit 2-O-(3*O*-carbamoyl-α-D-mannopyrannosyl)-L-gulopyranose and completion of the total synthesis of bleomycin A2. *J. Am. Chem. Soc. 116*, 5647–5656.
30. Piotto, M., Saudek, V., and Sklenar, V. (1992) Gradient-tailored excitation for single-quantum NMR spectroscopy of aqueous solutions. *J. Biomol. NMR 2*, 661–665.
31. Yan, J. L., Kline, A. D., Mo, H. P., Shapiro, M. J., and Zartler, E. R. (2003) The effect of relaxation on the epitope mapping by saturation transfer difference NMR. *J. Magn. Reson. 163*, 270–276.
32. Johnson, M. A., and Pinto, B. M. (2002) Saturation transfer difference 1D-TOCSY experiments to map the topography of oligosaccharides recognized by a monoclonal antibody directed against the cell-wall polysaccharide of group A *Streptococcus*. *J. Am. Chem. Soc. 124*, 15368–15374.
33. Meyer, M., and James, T. L. (2004) NMR-based characterization of phenothiazines as a RNA binding scaffold. *J. Am. Chem. Soc. 126*, 4453–4460.
34. Mayer, M., and James, T. L. (2002) Detecting ligand binding to a small RNA target via saturation transfer difference NMR experiments in D_2O and H_2O. *J. Am. Chem. Soc. 124*, 13376–13377.
35. Bhunia, A., Jayalakshmi, V., Benie, A. J., Schuster, O., Kelm, S., Krishna, N. R., and Peters, T. (2004) Saturation transfer difference NMR and computational modeling of a sialoadhesin-sialyl lactose complex. *Carbohydr. Res. 339*, 259–267.
36. Vold, R. L., Waugh, J. S., Klein, M. P., and Phelps, D. E. (1968) Measurement of spin relaxation in complex systems. *J. Chem. Phys. 48*, 3831.

BI702200M